Rigid-plastic analysis of tunnel face stability affected by ground water

S. Konishi & Y. Kawashima
Railway Technical Research Institute, Japan

T. Tamura
Kyoto University, Japan

T. Kitagawa & H. Iida
Japan railway Construction, Transport and Technology Agency, Japan

T. Matsunaga
Pacific Consultants Co. Ltd, Japan

ABSTRACT: The groundwater has significant influence on the stability of tunnel face. This report describes the method of evaluating tunnel face stability by a numerical analysis taking the above-mentioned effects into account. This method applies the finite element analysis (FEA) based on the plasticity theory, or the so-called rigid plastic finite element analysis (RPFEA). We improved the method so that water pressure can be taken into account. In this study, we consider the effect of draw-down of the groundwater level first by a nonmulti-element model of a two dimensional analysis (2DA). Next, we evaluate the face stability of an actual tunnel by a multi-element model of 2DA. The subject is a railway tunnel of Tohoku-Shinkansen, constructed in soft ground by the shotcrete tunneling method, or the currently so-called NATM. The ground water level is very high, while the over-burden is small. Moreover, it is difficult to draw down the groundwater level even by using the deep well method, since the ground near the face is heterogeneous and sandy with a clay layer. Because the tunnel face is unstable due to this condition, we evaluate the stability of the tunnel face by the proposed method.

1 INTRODUCTION

To ensure the tunnel face stability, which is normally subject to the influence of groundwater, it is effective to lower the groundwater level for tunnels constructed below the groundwater level.

This paper describes a method to evaluate the tunnel face stability by rigid plastic finite element analysis (RPFEA) giving consideration to the effects obtained by the above-mentioned method. In the analysis, the effect of groundwater on the tunnel face is expressed by applying a water pressure as a force on the ground.

2 ANALYSIS METHOD

2.1 *Rigid plastic finite element method*

Rigid plastic finite element analysis (RPFEA) pays attention only to the plastic state on the ground, and uses the upper bound theorem. Limit analysis is formulated by applying the FEA based on the plastic theory with this analysis. The method has attracted attention in the field of metal processing for the express purpose of calculating the magnitude of the force to process the metal (Hayes and Marcal, 1967). In geotechnical engineering, it can also be used as an analysis method in order to evaluate slope stability, stability of tunnel face and bearing capacity.

The method expresses only the state of the moment when plastic strain of the ground increases rapidly, or the state of the moment when the ground begins to break, and has some merits as shown below (Tamura et al. 1999; Konishi and Tamura, 2002).

- The elastic coefficient, which is useless under the critical state, is unnecessary.
- The method can well express the elastic flow near the critical state, of which errors become large with an elasto-plastic model.
- The initial stress is not required.

Basic equations for the analyses are as follows (Konishi et al. 2003; Tamura et al. 1984 and 1987).

(a) Equation of equilibrium

$$\sigma_{ij,j} + f_i = 0 \tag{1}$$

$\sigma_{ij,j}$: Total stress tensor
f_i : Nodal force

(b) Compatibility equation

$$\dot{\varepsilon}_{ij}=\frac{1}{2}\left(\dot{u}_{i,j}+\dot{u}_{j,i}\right) \tag{2}$$

$\dot{\varepsilon}_{ij}$: Strain rate tensor
$\dot{u}_i$: Nodal velocity vector

(c) Yield function and material constant

Drucker-Prager criterion is used as the yield function for the analysis.

$$f\left(\sigma_{ij}\right)=-\alpha I_1+\sqrt{J_2}=k \tag{3}$$

I_1 : First invariant of stress
J_2 : Second invariant of deviation stress
α, k : Material constants

The symbols α and k are derived as follows in the case of Mohr-Coulomb's failure criterion of the plane strain state.

$$\alpha=\frac{\sin\phi}{\sqrt{3\left(3+\sin^2\phi\right)}} \tag{4}$$

$$k=\frac{\sqrt{3}c\cos\phi}{3+\sin^2\phi} \tag{5}$$

ϕ : Internal friction angle
c : Cohesion of soil

(d) Kinematical constant

It is assumed that the yield function f is the potential of the plastic stress rate $\dot{\varepsilon}_{ij}$ in the case of the associated flow rule. The following conditions must be satisfied for the assumption to hold on the optional primary stress within the yield surface (principle of maximum plastic work).

- The plastic strain rate is an outward normal line on the yield surface.
- The yield surface must be a convexity.

The plastic strain rate $\dot{\varepsilon}_{ij}$ runs in the direction of the normal line of the yield surface, and is defined as:

$$\dot{\varepsilon}_{ij}=\Lambda\left(-\alpha\delta_{ij}+\frac{s_{ij}}{2\sqrt{J_2}}\right) \tag{6}$$

where δ_{ij} is the Kronecker's delta symbol.

If $\bar{\dot{e}}=\sqrt{\dot{\varepsilon}_{ij}\dot{\varepsilon}_{ij}}$ is assumed to be the equivalent magnitude of the plastic strain rate, the following equation is derived by squaring both sides of Equation (6).

$$\bar{\dot{e}}^2=\dot{\varepsilon}_{ij}\dot{\varepsilon}_{ij}=\Lambda^2\left(3\alpha^2+\frac{1}{2}\right) \tag{7}$$

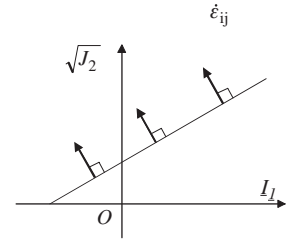

Figure 1. Indeterminate component of the Drucker-Prager criterion.

where Λ is obtained from Equation (7). When it is substituted into Equation (6), Equation (8) is derived as:

$$\frac{\dot{\varepsilon}_{ij}}{\bar{\dot{e}}}=\frac{\sqrt{2}}{\sqrt{6\alpha^2+1}}\left(-\alpha\delta_{ij}+\frac{s_{ij}}{2\sqrt{J_2}}\right) \tag{8}$$

Note that the isotropic component of Equation (8) is derived as:

$$\dot{\varepsilon}_{kk}+\frac{3\sqrt{2}\alpha\bar{\dot{e}}}{\sqrt{6\alpha^2+1}}=0 \tag{9}$$

where $\dot{\varepsilon}_{kk}$ means the volumetric component, which is a dilatancy, of the plastic strain rate.

Equation (9) can be rewritten as:

$$\dot{\varepsilon}_{ij}\left(\delta_{ij}+\frac{3\sqrt{2}\alpha}{\sqrt{6\alpha^2+1}}\frac{\dot{\varepsilon}_{ij}}{\bar{\dot{e}}}\right)=0 \tag{10}$$

The vector $\dot{\varepsilon}_{ij}$ is a perpendicular component to the yield surface of the Drucker-Prager criterion type, and others are parallel components. In other words, Equation (9) is a constraint condition for the plastic strain rate $\dot{\varepsilon}_{ij}$.

(e) Indeterminate component

Since an infinite number of the parallel components to the yield surface of the Drucker-Prager criterion exist on the surface even if the plastic strain rate $\dot{\varepsilon}_{ij}$ is given, the component is indeterminate (Figure 1). It is called the indeterminate stress.

(f) Relation between stress and strain rate based on the associated flow rule

The stress-strain rate relation will easily be derived if the stress δ_{ij} is decomposed into two parts, $\sigma_{ij}^{(1)}$ and $\sigma_{ij}^{(2)}$, where $\sigma_{ij}^{(1)}$ is the principal component defined to be parallel to the strain rate $\dot{\varepsilon}_{ij}$. On other hand, $\sigma_{ij}^{(2)}$, which is the indeterminate component, is defined to be a component parallel to the yield surface (Figure 2).

$$\sigma_{ij}=\sigma_{ij}^{(1)}+\sigma_{ij}^{(2)} \tag{11}$$

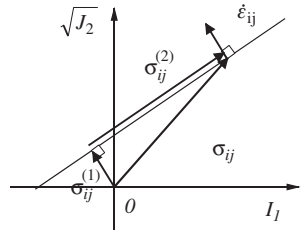

Figure 2. Relation between $\sigma_{ij}^{(1)}$ and $\sigma_{ij}^{(1)}$.

where $\sigma_{ij}^{(1)}$ and $\sigma_{ij}^{(2)}$ are derived as:

$$\sigma_{ij}^{(1)} = \gamma \frac{\dot{\varepsilon}_{ij}}{\dot{\bar{e}}} \tag{12}$$

$$\sigma_{ij}^{(2)} = \lambda \left(\delta_{ij} + \frac{3\sqrt{2}\alpha}{\sqrt{6\alpha^2+1}} \frac{\dot{\varepsilon}_{ij}}{\dot{\bar{e}}} \right) \tag{13}$$

γ : Positive constant
λ : Coefficient of indeterminate constant

The first invariant of stress I_1 and the second invariant of deviation stress J_2 in Equation (3) are calculated by using Equations (12) and (13). Since the front edge of the vector $\sigma_{ij}^{(1)}$ exists on the yield surface, the positive constant γ is obtained as follows by substituting I_1, J_2 and Equation (12) into Equation (3).

$$\gamma = \frac{\sqrt{2}k}{\sqrt{6\alpha^2+1}} \tag{14}$$

The constitutive equation for the rigid plastic of the Drucker-Prager criterion is derived as follows from Equations (11), (12), (13) and (14).

$$\sigma'_{ij} = \frac{\sqrt{2}k}{\sqrt{6\alpha^2+1}} \frac{\dot{\varepsilon}_{ij}}{\dot{\bar{e}}} + \lambda \left(\delta_{ij} + \frac{3\sqrt{2}\alpha}{\sqrt{6\alpha^2+1}} \frac{\dot{\varepsilon}_{ij}}{\dot{\bar{e}}} \right) \tag{15}$$

(g) Constraint on the velocity based on the upper boundary theorem

$$\int_V f_i \dot{u}_i dV + \int_{S\alpha} \overline{T}_i \dot{u}_i dS = 1 \tag{16}$$

where,
$\overline{T}_i$: Surface traction

(h) Relation between the stress and the pore water pressure

$$\sigma_m' = \sigma_m - \mu u \tag{17}$$

σ_m : Mean principal stress
σ'_m : Effective mean principal stress
μ : Pore water pressure
u : Load factor

(i) Effective stress
When the following symbols are used:

$$\sigma_{ij}' = s_{ij} + (\sigma_m - \mu u)\delta_{ij} \tag{18}$$

$\sigma'_{ij,j}$: Effective stress tensor
s_{ij} : Principal stress difference

The critical values of $\dot{u}_i$, λ and μ are derived by Equations (1), (2), (9), (15) and (16), with stresses is obtained from Equations (17) and (18).

2.2 *Groundwater and the effect of groundwater lowering*

When the following symbols are used, the fluctuation of unit weight of soil due to the fluctuation of the groundwater level is given by Equation (19),

$$\gamma_d = \rho_d g \tag{19}$$

γ_d : Unit weight of soil above the groundwater level

$$\gamma_{sat} = \frac{\rho_s - \rho_w}{1+e} g \tag{20}$$

γ_{sat} : Unit weight of soil under groundwater level
ρ_d : Dry density of soil
ρ_s : Density of saturated soil
ρ_w : Density of water
e : Void ratio

The effective stress and the strength of soil vary according to the unit weight of soil. In other words, the distribution of the unit weight of soil varies due to the fluctuation of ground water, while the effective stress increases or decreases in conformity with the equation of equilibrium. Since the strength of friction materials such as sandy soil changes with the fluctuation of the effective stress, changes of the groundwater level have an influence on the strength of the ground. Here, the yield condition is assumed to follow the Mohr-Coulomb's failure criterion, and the relation between strength and effective stress of the ground is examined. The groundwater level is configured based on the results of the seepage flow analysis, Dupuit-Forchheimer assumption or other study results. However, the groundwater level is assumed to be a straight line that connects the groundwater level of the observation well, which is located at a 20 m point ahead of the face, and the tunnel crown at the face for simplification in this paper.

The unit weight and the pore water pressure of the element must be approximated adequately, when the groundwater level exists on an element in the finite element analysis. This paper use the following approximating method.

If one of the elements and the groundwater level are assumed as shown in Figure 3, the water pressure on

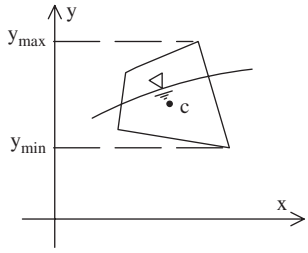

Figure 3. Method to set the self-weight of element and pore water pressure.

an element u_C is approximated as follows in the case where the element is under water completely.

$$u_C = \gamma_w (h_C - Y_C) \tag{21}$$

where,

Y_C : Y-axis of the barycentric coodinate of the element

h_C : Ground water level

In other words, Equation (21) is applied to each element as :

$$u_i = \gamma_w (h_i - Y_i) \qquad (i = 1, 2, 3, 4, , ,) \tag{22}$$

The mean water pressure of the element is derived as:

$$u_c = \frac{1}{4} \sum u_i \tag{23}$$

Note that the right-side of the above Equation determines only the sum of the pore pressure on the elements under the water.

Next, the self-weight of the element is derived as follows.

First, the coefficient α_r is determined from the ground water level of the barycentric coodinate, which is based on the minimum of the Y-axis value of the element, which is normalized by the Y-axis length of the element as:

$$\alpha_\gamma = \frac{h_c - y_{min}}{y_{max} - y_{min}} \tag{24}$$

Second, the self-weight of the element γ is derived after weighted by the coefficient as:

$$\gamma = (1 - \alpha_\gamma)\gamma_d + \alpha_\gamma \gamma_{sat} \tag{25}$$

2.3 *Evaluating method for the face stability*

RPFEA is applied with the Drucker-Prager criterion by assuming the associated flow rule. The unit weight of soil and water-pressure are treated as body force. In the analyses, the following three factors are taken into account.

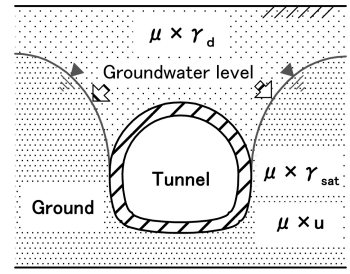

Figure 4. Relation between the load factor, the unit weight of soil, and pore water pressure.

- Changes in the unit weight of soil due to the change in the ground water level.
- Changes in the effective stress due to the change in the unit weight of soil and pore water pressure.
- Strength of the ground due to the change in the effective stress.

The stability of tunnel face is evaluated by acceleration μg as a face collapse occurs. The value of μg, in which g is the acceleration of gravity and μ is the load factor, is calculated by RPFEA. The method has the same test concept of tunnel face stability as that of the centrifuge test machine. Not only the unit weight of soil γ but also the pore water pressure u are multiplied by the load factor μ as a face collapse occurs. The load factor μ is an indication of the factor to the face stability. We considered that a face collapse actually occurs, when the load factor becomes $\mu \leq 1$. Then, we investigated the relation between the height of face and the ground water level at a face collapse by this method.

3 ANALYSIS BY SMALL-ELEMENT MODEL

RPFEA performs calculation 22-element model to establish the relation between the load factor and the ground water level. The model is assumes a circular tunnel (diameter D = 5.0 m) as a half-section of an actual tunnel since it is symmetrical. The analysis zones, at the upper and lower parts of the tunnel, are configured each as a 1D area. The lower end is fixed in the lateral and vertical directions, while, the side boundary, which is as 3D (=15.0 m) away from the tunnel-center line, is fixed only in the lateral directions, and free at the vertical directions (Figure 5). Table 1 shows the parameters for the analysis.

Figure 6 shows the relation between the ground water level H' which is normalized as dimensionless by the tunnel diameter and the load factor.

$$H' = \frac{H}{D} \tag{26}$$

Binding condition	Lower end	Side end
Lateral direction	Fix	Fix
Vertical direction	Fix	Free

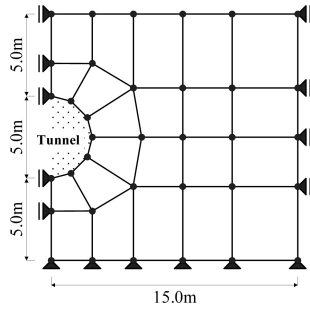

Figure 5. 22-element model for analysis.

Table 1. Parameters for analysis.

Parameters	Values
Unite weight of the water	$\gamma_w = 10\,\mathrm{KN/m^3}$
Saturated unite weight of the soil	$\gamma_{sat} = 20\,\mathrm{KN/m^3}$
Dry unite water of the soil	$\gamma_d = 15\,\mathrm{KN/m^3}$
Cohesion	$c = 10\,\mathrm{KPa}$
Internal friction angle	$\phi = 0°, 30°$

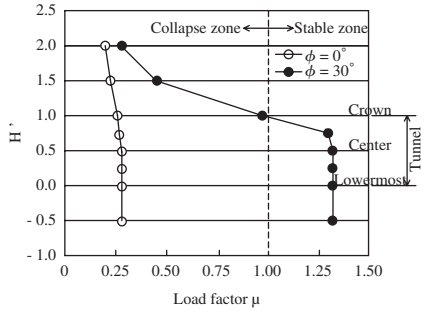

Figure 6. Analysis results of the 22-element model.

H' : Height of the ground water level which is normalized as dimensionless by the tunnel diameter

H : Height of the ground water level which is normalized as the tunnel diameter

D : Tunnel diameter.

As the reference point of the ground water level, the lowermost level of the tunnel is taken as the zero level. The face is stable when the groundwater lowers below the tunnel crown or the tunnel-center line in the lateral direction (hereinafter referred to as S.L.). The face where the internal friction angle is 30 degrees is more stable than where it is 0 degrees since the load factor increases as the groundwater level lowers. It is thought that the face is subjected more to the fluctuation of the effective stress as the internal friction angle becomes largely.

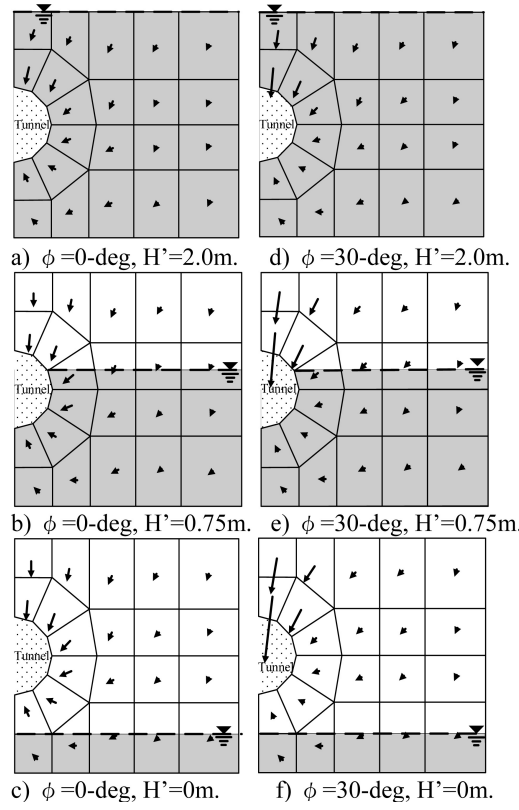

Figure 7. Velocity field at the face collapse of the 22-element model.

Figure 7 shows the velocity field at face collapse. It is much more likely to increase the velocity near the tunnel crown as the ground water level lowers when the internal friction angle is 30 degrees in particular. It is thought that shear resistance increases more in the upper ground than in the lower ground as the ground water level lowers.

4 SIMULATION ANALYSIS

4.1 *Outline*

Tohoku-Shinkansen is planed along the 675 km-route from Tokyo to Shin-Aomori, of which the section between Tokyo and Hachinohe has already been put in service. Construction work is now in full swing

to extend Tohoku-Shinkansen from Hachinohe to Shin-Aomori (82 km-route).

Twelve shallow tunnels have been planned or constructed in the soft ground between Hachinohe and Hakkoda Tunnel. Some of double-track Shinkansen tunnels are now under construction in the soft ground by the shotcrete tunneling method or the so-called New Austrian Tunneling Method (NATM).

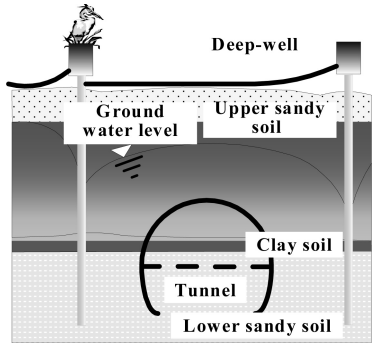

Figure 8. Situation of the actual tunnel.

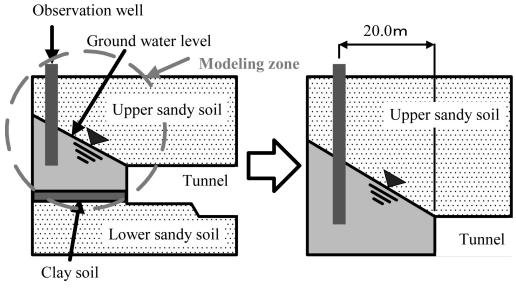

Figure 9. Analysis model.

Sambongihara-Tunnel is one of these tunnels. The geology near the face is alternation of strata formed from sandy soil and clay soil (Figure 8). The position of the clay soil at the face varies as the tunnel construction work advances. Moreover, the upper sandy soil was heterogeneous whereas the lower soil was homogeneous. Under these conditions, the ground water level in the lower sandy layer was fully lowered by the deep well method. Because it was difficult to lower the ground water level in the upper sandy layer, the face was unstable. In this paper, the face stability is evaluated by using the rigid plastic finite element analysis to ensure its integrity.

4.2 *Analysis model*

Sandy soil, in which the above clay soil exists at the observation point is modeled in the RPFEA (Figure 9). Parameters for analysis are the height of upper sandy soil at tunnel face, apparent cohesion and the ground water level at the observation well. The ground water level input at the 20 m point ahead of the face, because the pumping well is located at intervals of 20 m toward the tunnel axis.

The ground water level is assumed to be a straight line that connects the ground water level of the observation well, which is located at the 20 m point ahead of the face, and the tunnel crown at the face.

According to the observation results, the ground water level at the observation well is lowered almost linearly before the face approaches it. However, the ground water level was lowered only at the tunnel crown. Therefore, the ground water level is assumed to be a straight line in the models of this analysis.

4.3 *Analysis results*

Some results of the analyses are shown below. Figure 10 shows the relative distribution of velocity

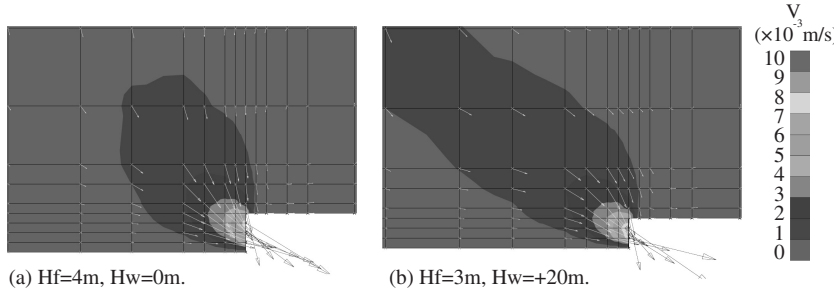

(a) Hf=4m, Hw=0m. (b) Hf=3m, Hw=+20m.

Hw : Difference between the ground water level at the 20m point ahead of the face and the level of the tunnel crown

Hf : Height of a face that can stand by itself

Figure 10. Velocity field at face collapse.

vectors of displacement at the moment when plastic strain increases abruptly. As the ground water level becomes higher, the ground movement toward the face changes into the lateral direction.

5 PROPOSAL OF A SIMPLE METHOD TO EVALUATE THE FACE STABILITY

A nomogram made up based on the results of RPFEA is proposed to simply evaluate the tunnel face stability. In the nomogram, lines are indices to evaluate the face stability. The left zone shows that the face is stable, whereas the right zone shows the condition of unstability (Figure 11).

Because the values of cohesion of sandy soil obtained by soil tests varied widely depending on the position and other conditions, several values of cohesion are input (Figure 12). The results indicate that cohesion influences face stability to a large extent. It is thought that the slant of the line expresses the effect of lowering ground water level on face stability. In other words, it is effective to lower the under ground water to the crown level, in order to ensure face stability. The results also show that the height of the face is effective for stability. Therefore, attention must be paid to the stability of the face, when the level of the clay layer goes down.

Next, construction results are input in the nomogram to evaluate the adequacy of analysis. Table 2 shows construction results. When clay soil exists over the entire face (section number No.3), it shows that the face is stable according to the construction results in the nomogram. On the other hand, when an alternation of strata with sandy soil and clay soil is formed at the face (section number No.1), the face is unstable. Since the nomogram based on the analysis coincides with the construction results, it is effective to evaluate the face stability by using the nomogram.

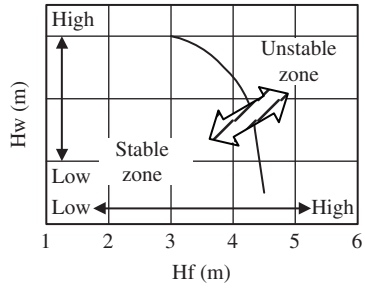

Figure 11. Concept of nomogram.

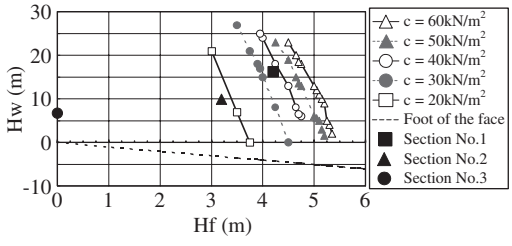

Figure 12. Proposed nomogram.

Table 2. Construction results.

Section number	Geological condition	Hf (m)	Face stability	Hw (m)
No. 1	Alternation of strata	4.2	Unstable	16.2
No. 2	Alternation of strata	3.2	A little unstable	9.9
No. 3	Clay soil	0	Stable	6.7

6 CONCLUSIONS

- It becomes clear that it is possible to evaluate the face stability, which is affected by the ground water, by applying RPFEA while giving consideration to the effects obtained by the groundwater.
- It is confirmed that three factors concerning the lowered groundwater level are effective to evaluate the face stability. These factors are the fluctuation of the unit weight of soil due to the fluctuation of the groundwater level, fluctuation of the effective stress caused by the fluctuation of the unit weight of soil and pore water pressure, and fluctuation in the strength of the ground induced by the fluctuation of the effective stress.

We will compare analysis results and construction data, and study the methods to evaluate cohesion, set an appropriate groundwater level and create an optimum model in the future.

REFERENCES

Hayes, D.J. & Marcal, P.V. 1967. Determination of upper bounds for problems in plane stress using finite element techniques. *Int. J. Mech. Sci., Vol.9*: 245–251.

Tamura, T., Adachi, N., Konishi, S. & Tsuji, T. 1999. Rigid-plastic finite element method for frictional materials. *Journal of geotechnical engineering, JSCE, No.638/3-49*: 301–310. (In Japanese)

Konishi, S. & Tamura, T. 2002. Evaluation of tunnel face stability in sandy ground with clay layers. *Journal of Geotechnical Aspects of underground construction in soft*

ground, 3rd international symposium IS-Toulouse, ISSM and TC28, 6th session: 53–58.

Konishi, S., Nishiyama, T., Tamura, T., Iida, H. & Tadenuma, Y. October 2003. Evaluation of Tunnel Face Stability Affected by Ground Water. *Proceedings of he International Workshop on Prediction and Simulation Methods in Geomechanics, IWS-Athens*: 177–180.

Tamura, T., Kobayashi, S. & Sumi, T. 1984. *Limit analysis of soil structure by rigid plastic finite element method. Soils and Foundations, JSSMFE, Vol.24, No.1, pp.34–42.*

Tamura, T., Kobayashi, S. & Sumi, T. 1987. Rigid-plastic finite element method for frictional materials. *Soils and Foundations, JSSMFE, Vol.27, No.3, pp.1–12.*